

# **3rd International Conference Advanced Mechanics: Structure, Materials, Tribology**

---

## **Indentation of Axisymmetric Bodies into a Plastic Half-Space**

AIPCP25-CF-AMSMT2025-00015 | Article

Submitted on: 24-12-2025

PDF auto-generated using **ReView**



# Indentation of Axisymmetric Bodies into a Plastic Half-Space

Israel Karimov<sup>1, a)</sup>, Ismail Safarov<sup>1, b)</sup>, Muhsin Teshayev<sup>2, c)</sup>,  
Akhtam Rustamov<sup>3, d)</sup>

<sup>1</sup>*Tashkent Chemical-Technological Institute, Uzbekistan*

<sup>2</sup>*Branch of the Institute of Mathematics named after V.I. Romanovsky of the Academy of Sciences of the Republic of Uzbekistan, Uzbekistan*

<sup>3</sup>*Navoi State Pedagogical University, Uzbekistan.*

<sup>a)</sup> Corresponding author: israel.karimov@mail.ru  
<sup>b)</sup> safarov54@mail.ru  
<sup>c)</sup> muhsin\_5@mail.ru  
<sup>d)</sup> akhtamrustamov@gmail.com

**Abstract.** The process of an axisymmetric introduction of absolutely rigid bodies of rotation in an ideal rigid-plastic half-space is studied in the framework of the present paper. The yield condition of Tresca and the corresponding flow law are considered and in this way we can describe the plastic zone that starts when ultimate indentation force is apparent. To address the issue, the characterization technique is applied to come up with the field of slip lines and find out the distribution of stress and velocity in plastic region. The paper takes into account an effect of friction coefficient, die shape (cone, ball, cylinder with a flat base) and alterations of the free surface shape to the value of the ultimate pressure. The results of numerical analysis are compared with the known experimental data and showed good agreement, which confirms the correctness of the model. The principles of complete and incomplete plasticity are reexamined and conversion between plastic and elastic states are examined. The resulting solutions show the development of the area of plasticity and the effects of the parameters on the final load.

## INTRODUCTION

Issues of contact interaction and die embedding in a deformable medium are classical issues of continuum mechanics and plasticity [1, 2, 3]. They are practically significant to the work of hardness testing of materials, stamping, pressing, and other technologies of pressure processing. A major addition to the axisymmetric plasticity problem solution was made by A.Y. Ishlinsky [4] who was the first to use the characterization approach to the Brinell sample problem, with very good agreement between theory and experiment. The model of an ideal rigid-plastic body is used in the paper because the stresses in the body meet the Tresca yield criterion, and the strains meet the flow law. Of special concern are states of full and incomplete plasticity in the light of the influences of friction and changes in free surfaces. Hyperbolic systems of equations are solved by numerical techniques like the method of characteristics and successive approximations. Examination of the stress-strain state arising under the indenter is used to identify the mechanical properties of materials, predict their destruction and optimize technological processes. Particular cases of cone, ball and cylinder embedding are explored, with an examination of the impact of friction coefficient and embedding depth upon the final load. The aim of the current work is to develop analytical and numerical model of axisymmetric introduction of bodies of rotation of different shapes into an ideal plastic half-space and to observe the effect of friction, die shape and free surface deformation on the nature of plastic flow.

## MATERIAL AND METHODS

We consider an ideal rigid-plastic medium for which the deformations obey the Tresk yield condition. The cylindrical coordinate system  $(r, \varphi, z)$  is used, and the axial symmetry of the problem is assumed: the stress components  $\sigma_r, \sigma_z, \tau_{rz}$  and strain rates depend only on the  $r$  and  $z$  coordinates. The relationship between the components of the stress and strain rate tensors is determined using the associated flow law. The analysis of flows in different modes corresponding to the faces and edges of the Tresk prism was carried out by R. Schild [5]. The system of equations corresponding to the regime  $\sigma_\varphi = \sigma_1$  for the stress state was studied by Genki. This system consists of the differential equations of equilibrium, the plasticity condition  $\sigma_1 - \sigma_3 = 2\tau_s$  and the equality  $\sigma_\varphi = \sigma_1$ . Using the Levy transformation

$$\sigma_r = p - \tau_s \sin 2\theta; \sigma_z = p + \tau_s \sin 2\theta; \tau_{rz} = \tau_s \cos 2\theta,$$

where  $p = (\sigma_r + \sigma_z)/2$ ,  $\theta = (l, r) - \pi/4$ ,  $(l, r)$  is the angle between the first principal direction and the  $Or$  axis, the equations of equilibrium take the following form with respect to the unknown functions  $p$ :

$$\begin{aligned} \frac{\partial p}{\partial r} - 2\tau_s \frac{\partial}{\partial \varphi} \left( \frac{\partial q}{\partial r} + \sin 2\theta \frac{\partial q}{\partial z} \right) &= \frac{\tau_s}{r} (1 + \sin 2\theta), \\ \frac{\partial p}{\partial z} - 2\tau_s \frac{\partial}{\partial \varphi} \left( \frac{\partial q}{\partial z} - \cos 2\theta \frac{\partial q}{\partial r} \right) &= \frac{\tau_s}{r} \cos 2\theta. \end{aligned}$$

As it is known [6], this system is hyperbolic and has two families of characteristic lines coinciding with slip lines (a slip line is a line tangent at each point to which coincides with the area of maximum tangential stress).

Along the characteristic lines for the determination of  $p, \theta$  there are the relations

$$\begin{cases} d(p - q) = \frac{dr + dz}{2}, & \text{on the } a \text{ line,} \\ d(p + q) = \frac{dr - dz}{2}, & \text{on the } b \text{ line.} \end{cases}$$

Here and hereafter, all stresses are referred to  $2\tau_s$ . The velocities  $v_r, v_z$  are found from the incompressibility conditions and the condition of coaxiality of stress and strain rate tensors. The system of equations with respect to the two unknowns  $v_r, v_z$  also belongs to the hyperbolic type, and its characteristics coincide with the slip lines.

$$\begin{cases} du - v dq = -\frac{udr - v dz}{2r}, & \text{on the } a \text{ line,} \\ dv + u dq = -\frac{udz + v dr}{2r}, & \text{on the } b \text{ line.} \end{cases}$$

where  $u, v$  are displacement velocities along and - slip lines, respectively. The constraints from the flow law ensure the consistency of stress and velocity fields.

The slip line field is constructed numerically, starting from the boundaries where stresses (e.g., on the free surface) or friction conditions (on the contact surface) are known. The plastic deformation region is partitioned into a grid, at the nodes of which the values of  $p, \theta, v_r$  and  $v_z$  are iteratively determined.

Friction accounting and boundary conditions. On the contact surface between the indenter and the medium, Coulomb's law of dry friction is taken into account, which limits the tangential stress  $\tau_n$  to a value proportional to the normal stress  $\sigma_n$  ( $|\tau_n| \leq m|\sigma_n|$ ), where  $m$  is the coefficient of friction. When the maximum value ( $\tau_n = 0.5$ ) is reached, the so-called "sticking" occurs. These conditions determine the angle of the slip lines at the contact surface. When the body is partially roughened, a stagnant area is formed - an area that moves with the body. The size of the zone depends on the coefficient of friction and shape. The zone boundary is defined by the slip line intersecting the axis under /4.

A state of incomplete plasticity. In the process of indentation, the material undergoes a transition from an elastic state to a plastic state. The model based on the Haar-Karman hypothesis [7, 8] allows us to distinguish between two states:

Incomplete plasticity. The Tresca yield condition ( $\sigma_1 - \sigma_3 = 1$ ) is satisfied, but the intermediate principal stress  $\sigma_2$  is strictly between  $\sigma_1$  and  $\sigma_3$  ( $\sigma_1 > \sigma_2 > \sigma_3$ ). In this state the deformations along the  $\sigma_2$  direction are elastic:

$$s_2 = \frac{3K}{1+n} \dot{\varepsilon} e + (1-2n)e_2 \dot{u}$$

where  $K$  is the bulk compression modulus referred to  $2\tau_s$ ,  $v$  is the Poisson's ratio,  $\varepsilon$  is the volume strain.

Full plasticity. The additional condition  $\sigma_2 = \sigma_1$  or  $\sigma_2 = \sigma_3$  is fulfilled. All deformations become plastic.

System of equations of incomplete plasticity

$$\begin{aligned} \frac{p}{r} - \cos 2q \frac{q}{r} - \sin 2q \frac{q}{z} &= \frac{1}{r} \frac{\sin 2q}{2} - 3(p - K_e) \dot{u} \\ \frac{p}{z} - \sin 2q \frac{q}{r} + \cos 2q \frac{q}{z} &= - \frac{\cos 2q}{2r}, \\ \frac{u_r}{r} - \frac{u_z}{z} \cos 2q + \frac{u_r}{z} + \frac{u_z}{r} \sin 2q &= 0, \\ \frac{u_r}{r} + \frac{u_z}{z} + 2n \frac{u_z}{r} &= \frac{2(1+n)}{3K} p. \end{aligned}$$

is solved by the method of successive approximations starting from the full plastic solution. Iterations are continued until convergence of the force on the die.

## RESULTS AND DISCUSSION

Construction of slip line meshes. Based on the methodology outlined in the source material, slip line meshes were constructed for different types of indenters:

Slip line fields were calculated for the smooth and rough cone (Fig. 1).

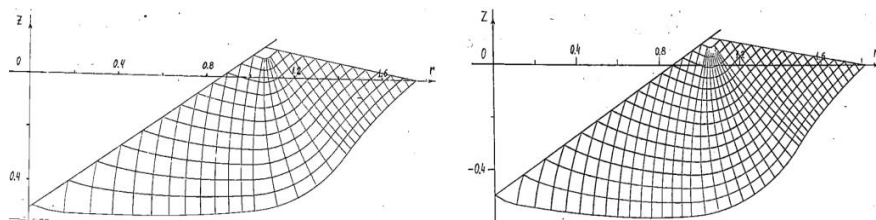


FIGURE 1. Grid of slip lines for smooth and rough ( $m=0.05$ ) cone

Calculations have shown that this algorithm works for a wide range of variation in the values of angle  $\beta$  and friction coefficient  $m$ , but for angles smaller than  $50^\circ$  the consistency of stress and velocity fields is not fulfilled. This means that the condition of full plasticity for such angles is not realized in the whole plastic region.

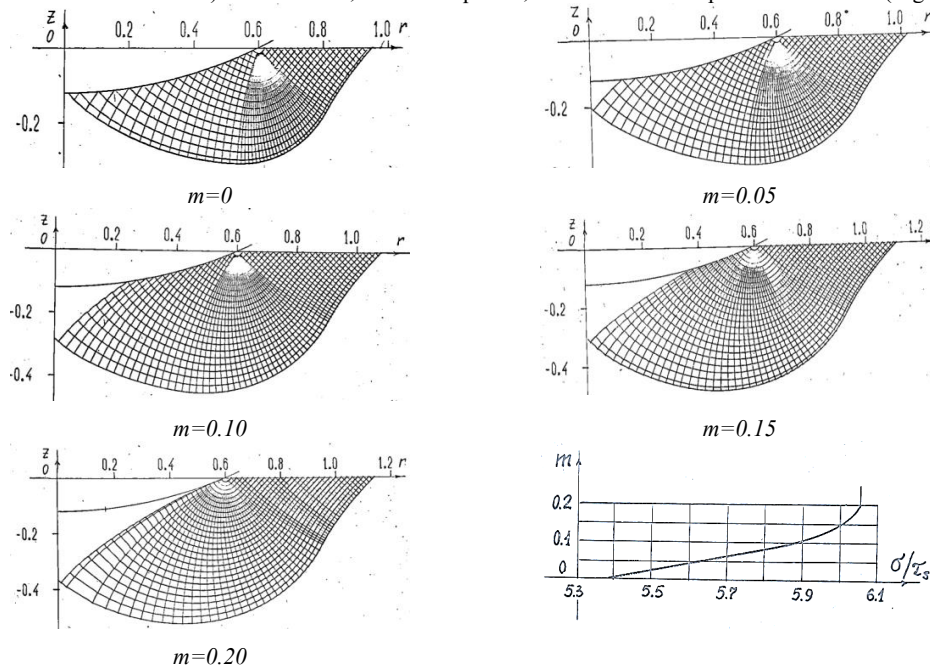
Comparison of the calculated data with the experimental results of Dugdale [9] for half-shell angles of  $50^\circ$  and  $60^\circ$  showed good agreement (Table 1).

TABLE 1. Comparison of calculated data with experimental data

	$\beta = 50^\circ$		$\beta = 60^\circ$	
	Experiment	Calculation	Experiment	Calculation
$\frac{\sigma}{2\tau_s}$	2,13 (Fe) 2,29 (Cu) 2,24 (Al)	a) 2,37 b) 2,14	2,18 (Fe) 2,47 (Cu) 2,40 (Al)	a) 2,48 b) 2,30
$\frac{h \cdot 100}{2r}$	6,90 (Fe) 8,47 (Cu) 9,02 (Al)	7,33	4,08 (Fe) 5,80 (Cu) 6,67 (Al)	5,36
$\frac{r_L}{r}$	2,20 (Fe) 1,53 (Cu) 1,65 (Al)	1,72	1,76 (Fe) 1,53 (Cu) 1,43 (Al)	1,65

In Table 1, letter (a) means the average pressure for the cone without taking into account the change of the free surface; (b) corresponds to the average pressure calculated by the above algorithm.  $h$  is the height of the bulging part of the medium, counted from the initial level;  $r$  is the cone radius at the level of intersection of the cone surface with the free surface;  $r_L$  is the maximum radius of the plastic region.

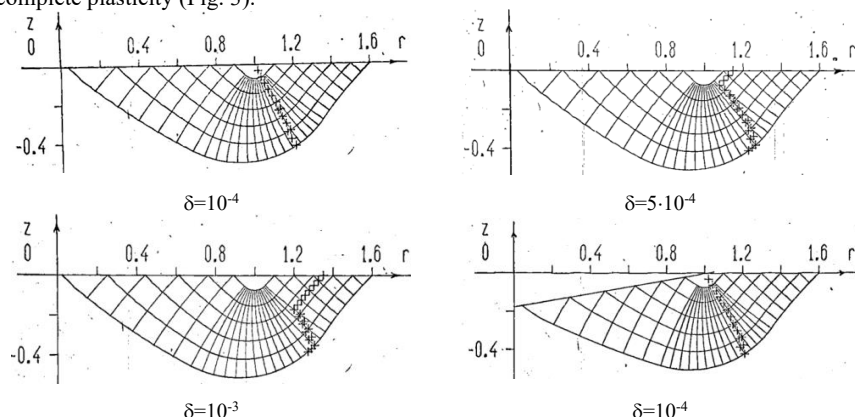
Calculations were performed for ball indentation at different friction coefficients ( $m = 0; 0.05; 0.1; 0.15; 0.2$ ). It was found that as the coefficient of friction increases, the volume of the stagnant zone (the area under the indenter that moves with it as a unit) increases and, as a consequence, the mean ultimate pressure increases (Fig. 2).



**FIGURE 2.** A grid of slip lines for smooth and rough ball.  
Dependence of average pressure on the value of friction coefficient

The mesh analysis shows that the indenter geometry and the friction coefficient on the contact surface dramatically affect the plastic flow pattern of the material. In particular, the presence of friction leads to distortion of slip lines at the indenter surface and formation of stagnant zones.

States of complete and incomplete plasticity. The regions of complete and incomplete plasticity are separated by surfaces where  $\sigma_2$  becomes equal to one of the extreme principal stresses. Calculations show that with increasing depth of introduction the region of incomplete plasticity decreases, and eventually the entire plastic zone passes to the state of complete plasticity (Fig. 3).



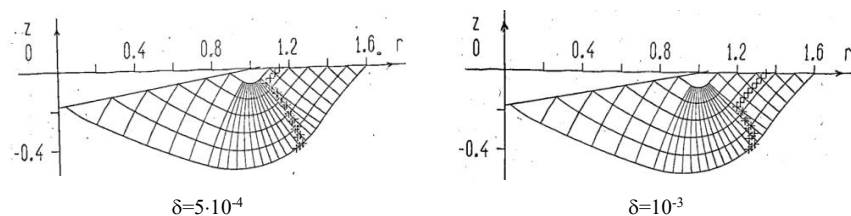


**FIGURE 3.** Grid of slip lines and boundary of zones of complete and incomplete plasticity

The initial isotropic material becomes anisotropic during plastic deformation. This occurs due to the formation of a mesh of weakened sliding surfaces. Shear resistance along these surfaces drops, while elastic coupling is maintained in other directions. This deformational nature of anisotropy is a key feature of the plastic behavior of materials.

## CONCLUSION

The conducted study confirmed that the method of characteristics is an effective tool for solving problems of axisymmetric introduction of bodies of rotation into plastic medium. Despite idealizing assumptions (rigid-plastic material model), this approach allows to describe with high accuracy key aspects of the indentation process: formation of plastic zones, influence of indenter geometry and friction, and occurrence of stagnant zones. The obtained results can be used in engineering calculations and for verification of numerical methods.

## REFERENCES

1. H. Hencky, “Über einige statisch bestimmte Fälle des Gleichgewichts in plastischen Körpern.” (1923), ZAMM **3** (4): 241–251. <https://doi.org/10.1002/zamm.19230030401>
2. L. Prandtl, O tvyordosti plasticheskikh materialov i sопротивлениi rezaniyu [On the hardness of plastic materials and resistance to cutting], in Teoriya plastichnosti [Theory of Plasticity] (IL, Moscow, 1948), pp. 70–79.
3. R. Hill, The Mathematical Theory of Plasticity (Oxford University Press, Oxford, 1950).
4. A. L. Ishlinsky, “The problem of plasticity with axial symmetry and Brinell’s test.” *J. Appl. Math. Mech.* **8**, pp. 201–224 (1944).
5. R. T. Shield, “On the plastic flow of metals under conditions of axial symmetry.” Proc. R. Soc. London, Ser. A **233** (1193), pp. 267–287 (1955). <https://doi.org/10.1098/rspa.1955.0262>
6. D. D. Ivlev, The Theory of Ideal Plasticity (Nauka, Moscow, 1966).
7. A. Haar and T. von Kármán, “Zur theorie der spannungszustände in plastischen und sandartigen medien.” *Nachr Gesellsch Wissensch öttingen, Math-phys Klasse* 1909: 204–218.
8. S. A. Khristianovich & E. I. Shemyakin, On the theory of ideal plasticity. *Mechanics of Solids*, **4**, pp. 86–97, (1967).
9. D. S. Dugdale, Cone Indentation Experiments. *Journal of the Mechanics and Physics of Solids*, **2**(4), pp. 265–277 (1954). [https://doi.org/10.1016/0022-5096\(54\)90015-0](https://doi.org/10.1016/0022-5096(54)90015-0)